Proceedings of the 10th International Conference on Heat Transfer and Fluid Flow (HTFF'23)
Brunel University, London, United Kingdom –August 06-08, 2023
Paper No. HTFF 200
DOI: 10.11159/htff23.200

Effect of Surface Wettability on Nucleate Pool Boiling Under Low Gravity Conditions

Abhishek K. Sharma*, Shaligram Tiwari
Department of Mechanical Engineering
Indian Institute of Technology Madras, Chennai-600036, India
Email: erabhisunny@gmail.com

Abstract **-** Surface wettability plays a significant role in determining the heat transfer characteristics associated with a growing bubble in nucleate pool boiling (NPB). Most of the prior works have considered the growth of the bubble under terrestrial gravity conditions. The process of NPB can also be employed as a promising method for heat transfer in devices and equipment working under low gravity conditions. The advancement in computational techniques offers improvement to numerically investigate the impact of surface wettability on NPB heat transfer at various gravity levels so as to design the enhanced surface in a rational manner. The present work focuses on the growth and detachment of a bubble on a horizontal surface with varying wettability in order to understand its contribution on heat transfer process at different gravity levels. The computational domain consists of two regions. The interface between the liquid and vapor in the macro-region has been captured by the VOF method. Micro-layer evaporation underneath the bubble base has a significant contribution on overall heat transfer to the vapor bubble in the process of NPB. This has been calculated on the basis of conductive heat transfer model. The phase change process is modeled by using 'saturated-interface-volume' phase change model. Water has been taken as the working fluid in the current study. The influence of surface wettability on bubble morphology and associated heat transfer behaviour has been investigated at different values of gravity levels. Computations have been performed by providing different heat flux (q) to the heating surface in order to study the effect of gravity level and contact angle (C_a) on bubble growth and heat transfer. It has been found that the impact of wettability modulation is more pronounced for weakly wetted surfaces at higher q value under relatively low gravity conditions.

Keywords**:** Nucleate pool boiling, wettability modulation, Micro-layer evaporation, Bubble morphology, VOF method

1. Introduction

NPB is a widely accepted mode of heat transfer due to its capability of transferring large amount of heat within a low superheat value. It finds its application in many areas, including chemical industries, nuclear power plants and refrigeration systems. Nucleation, bubble growth and departure characterise the process of NPB, which is a complex phenomenon affected by various parameters including surface wettability, local heat conditions and gravity levels. In order to take advantage of NPB for equipment working under low gravity conditions, it is reasonable to investigate the effect of wettability modulation under different heating conditions and gravity levels. Several studies have been performed in order to find empirical correlations and models for different bubble dynamics parameters that govern the heat transfer process during NPB. Lee and Nydahl [1] carried out the numerical simulation to explore the formation of a bubble in a simple manner, assuming the bubble to have a hemispherical shape. Son et al. [2] experimentally and numerically studied the dynamics of bubble on a horizontal surface. They used finite difference approach with level set method in order to consider the effect of phase change at the liquid-vapor interface. It has been reported that the bubble size increases with the increment in superheat level and C_a. To account for the effect of surface wettability and fluid characteristics, Abarajith and Dhir [3] performed a numerical study considering two different fluids water and PF-5060. They found that the increment in bubble departure diameter (D_d) with an increase in C_a is comparatively more for the case of water. Using level set method, Wu and Dhir [4] studied the effect of subcooling under microgravity conditions and reported an enhancement in influence of subcooling on bubble size under microgravity as compared to normal gravity conditions. Wu and Dhir [5] further extended this work to analyze the impact of non-condensable gases on heat transfer and bubble dynamics and found that the velocity of the liquid surrounding the bubble gets altered due to the effect of noncondensables. Using Lattice Boltzmann Method (LBM), Gong and Chang [6] numerically investigated the effect of superheat, surface wettability and heater size on pool boiling behavior under saturated condition. They observed an enhancement in the nucleation site density with the rise in heater size, superheat level and C_a. Pandey et al. [7] numerically explored the process of NPB on a horizontal surface using CLSVOF method of interface capturing with a modified micro-layer evaporation model. They have obtained power law curve for predicting the dependency of bubble growth on wall

superheat temperature by comparing the obtained result with the analytical and experimental data.The present work attempts to study the effect of wettability modulation on NPB under low gravity conditions at various heat flux (q) values. For this hydrophilic surface is considered, which is further characterised as strong and weak wettability surfaces on the basis of contact angle between the heating surface and the bubble. Weak wettability surface (WWS) is defined as that for which C_a lies between 45° to 90° whereas for strong wettability surface (SWS), C_a lies in the range of 0° to 45°.

2. Methodology

2.1 Governing Equations

The VOF method given by Hirt and Nichols [8] is used in order to capture the vapor-liquid interface. Volume fraction of liquid and vapor in each cell is represented by α_l and α_v respectively. In the two-phase cell, mass conservation is achieved by solving the following equations.

$$\frac{\partial \alpha_l}{\partial t} + \nabla.(U\alpha_l) = \frac{1}{\rho_l}\dot{m}_l \quad (1)$$

$$\frac{\partial \alpha_v}{\partial t} + \nabla.(U\alpha_v) = \frac{1}{\rho_v}\dot{m}_v \quad (2)$$

where U, $\dot{m}$ and ρ are the velocity vector, volumetric mass flow rate and density, respectively. l and v represents the liquid and vapor phase. On the basis of single fluid flow formulation and utilizing the surface tension model given by Brackbill et al. [9], the momentum equation is modified as follows

$$\frac{\partial}{\partial t}(\rho(U) + \nabla.(\rho UU) = -\nabla p + \rho g + \nabla.[\mu(\nabla U + \nabla U^T)] + \sigma k\hat{n}\delta_s \quad (3)$$

where μ, and σ are viscosity and surface tension coefficient respectively. $\hat{n}$ is unit vector normal to the interface and k is the interface curvature. The contribution of micro-layer evaporation is taken as a source term (S_e) in the following energy equation

$$\frac{\partial}{\partial t}(\rho E) + \nabla.\big(U(\rho E + p)\big) = \nabla.\mu(\lambda\nabla T) + S_e \quad (4)$$

Thermo physical are calculated as follows

$$\rho = \rho_v\alpha_v + \rho_l\alpha_l \quad (5)$$

$$\mu = \mu_v\alpha_v + \mu_l\alpha_l \quad (6)$$

$$\lambda = \lambda_v\alpha_v + \lambda_l\alpha_l \quad (7)$$

where λ, T, P, E and S_e represents the thermal conductivity, temperature, pressure, energy and source term, respectively. The effect of micro-layer evaporation is calculated separately using the micro-layer model given by Cooper and Lloyd [10]. According to this model, the initial micro-layer thickness at a particular radial location is given as

$$\delta_0 = 0.8\sqrt{\vartheta t_R} \quad (8)$$

where t_R is the time taken by the contact line to travel to the radial location at which initial micro-layer thickness is required. ϑ is the kinematic viscosity. Micro-layer heat transfer is computed by using conductive heat transfer model.

$$q_{ml} = \lambda_l \frac{T_w - T_{sat}}{\delta(r)} \quad (9)$$

where q_{ml} is the local heat transfer through the micro-layer and $\delta(r)$ is the local thickness of micro-layer.

Phase change model based on saturated-interface-volume is used to account for the phase change process at vapor-liquid interface in the macroscopic region.

2.2 Computation domain and boundary conditions

Two-dimensional axis-symmetric domain is used to perform the computations in the present study.The height and radius radius of the domain are 8 mm and 4 mm respectively. Here phases are defined on the basis of vapor volume fraction. In Fig. In Fig. 1, liquid phase is represented by blue colour where vapor fraction is zero and vapor is shown in the red colour where where vapor fraction is 1.Heating surface and outer radial wall are subjected to no-slip boundary condition. The boundary at boundary at the outlet is maintained at atmospheric pressure by applying pressure outlet boundary condition.

2.3 Numerical Technique

The present computational work is carried out by using VOF method incorporated in commercial software ANSYS Fluent 2021 R1. User defined function (UDF) is used to consider the effect of micro-layer evaporation. Geo-Reconstruct method is utilized for solving volume fraction equation. Pressure-velocity coupling is done by PISO algorithm. Energy and momentum equations are discretized by second-order upwind scheme while PRESTO! scheme is used for the discretization of pressure. Gradients are calculated by employing least square cell-based method

2.4 Grid Independence Study

Three different grid sizes are taken to perform the grid independence study and the result obtained in the form of bubble departure diameter is compared for all the three cases.

Table 1: Grid independence study

Case	Minimum edge length(mm)	No. of cells	Bubble departure diameter(mm)
1	0.012	220780	1.757
2	0.01	318801	1.64
3	0.008	498501	1.635

It is evident from Table 1 that the departure diameter for the second and third case is very close as compared to that for the first and second case. So, in order to obtain accurate results with optimum computational cost, grid size of 0.01mm with 318801 number of cells is chosen to perform further computations in the present work. Time step of 10^{-6} is found to be accurate for the current study.

2.5 Validation

In order to validate the present numerical procedure, experimental and numerical results of Allred et al.[11,12] are used in which they have considered hydrophilic surface with a small value of contact angle. Results are compared in form of bubble morphological evolution with normalized time t* (bubble growth time/departure time). It can be seen from Fig. 2 that the variation of bubble morphology for the present work follow the same trend as that was observed in the previous work of Allred et al. [11,12].

3. Results and Discussion

3.1 Bubble Morphology

Figures 3 - 6 show the progression of bubble morphology during the bubble growth. The variation in morphology of the bubble at different contact angles (C_a) for heat flux (q) of 30 kW/m^2 under a gravity level of 0.8 g is shown in Fig. 3. As it can be observed that the departure of the bubble at lower C_a is faster as compared to higher C_a. The difference in bubble departure diameter (D_t) for SWS with the change in C_a value by 10° is 30 ms which is more as compared to the corresponding change for WWS which is 18 ms. The lower surface of the departed bubble changes from concave to flat as the wettability of the surface decreases.

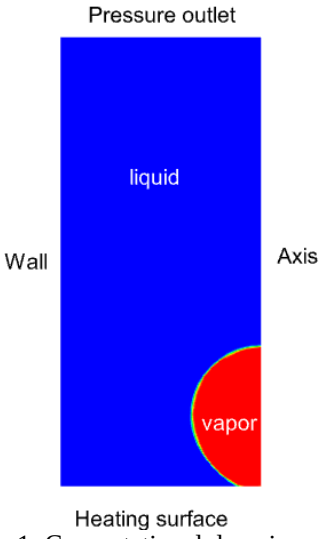

Fig. 1: Computational domain

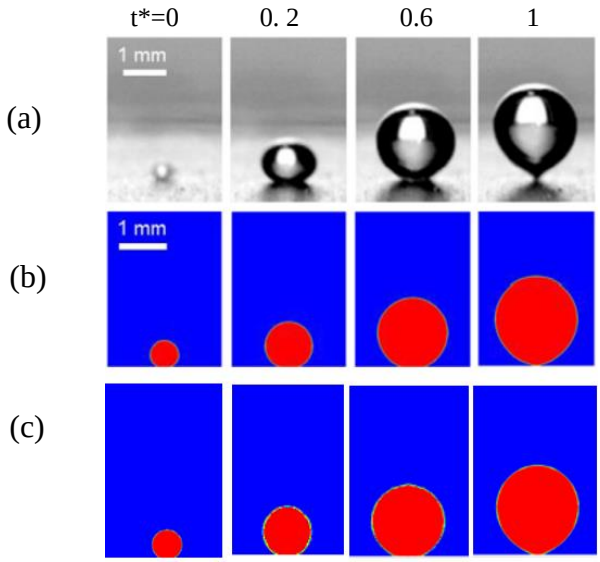

Fig. 2: Progression of bubble morphology with normalized time (a) experimental Allred et al. [11] (b) numerical Allred et al. [12] (c) present work

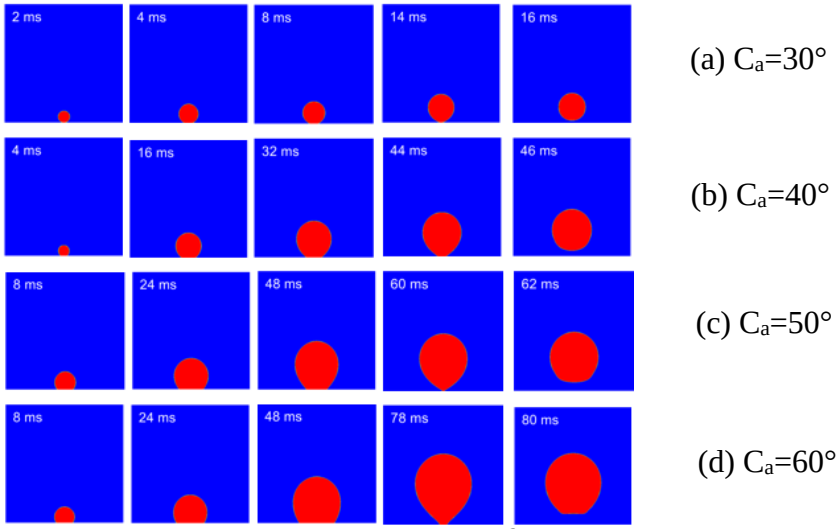

Fig. 3: Progression of bubble morphology for q of 30 kW/m^2 at gravity level of 0.8 g

Figure 4 depicts the bubble morphology for surfaces with different wettability at a q value of 30 kW/m2 under gravity level of 0.4g. It can be seen from Fig. 4 that the Dt for SWS increases by 46 ms whereas for WWS this value decreases by 2 ms with the increase in Ca by 10° in each case. This demonstrates that the reduction in wettability leads to an increment in Dt for SWS in a more significant manner. In contrast, for the WWS, this effect gets reversed with a slight difference in Dt as the gravity level is further reduced. The change in the shape of lower surface of the departed bubble with the increment in Ca follows the similar pattern as that is being observed at relatively higher gravity level (0.8 g), showing that the reduction in gravity level at lower q value does not create significant influence on the shape of the lower part of the departed bubble for the contact angles considered in the present study.

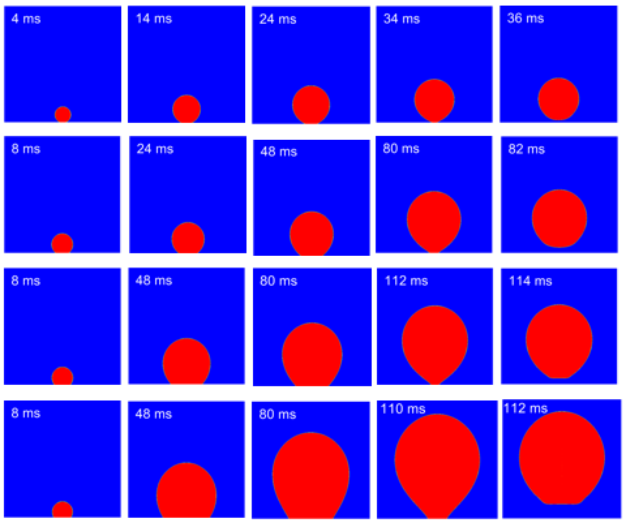

(a) C_a=30°

(b) C_a=40°

(c) C_a=50°

(d) C_a=60°

Fig. 4: Progression of bubble morphology for q of 30 kW/m^2 at gravity level of 0.4

For the q value of 40 kW/m^2 and gravity level of 0.8g, morphological evolution of the bubble for surfaces with different wettability is shown in Fig. 5. On comparing the above results with the corresponding bubble morphology at lower heat flux value (Fig. 3), it can be stated that the difference in D_t with the increase in C_a value by 10° is nearly same for SWS which is 30 ms at both heat flux values whereas for WWS this gap in D_t gets reduced which is 18 ms at the lower heat flux and 2 ms for higher heat flux value.

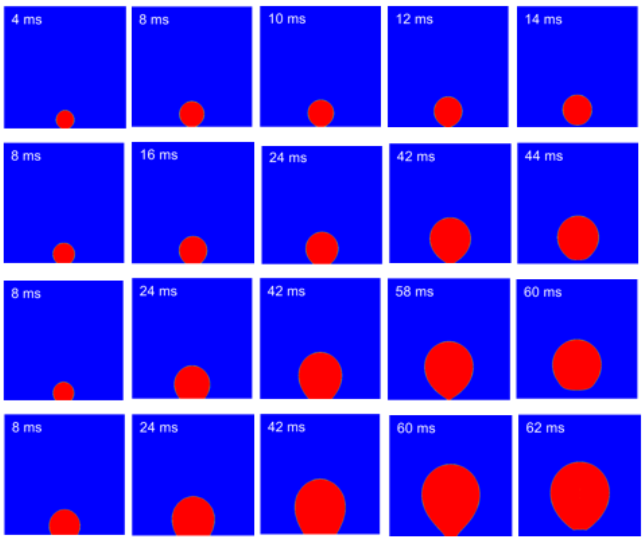

(a) C_a=30°

(b) C_a=40°

(c) C_a=50°

(d) C_a=60°

Fig. 5: Progression of bubble morphology for q of 40 kW/m^2 at gravity level of 0.8 g

Under the gravity level of 0.4 g and q value of 40 kW/m^2, growth process of the bubble with wettability modulation is presented in Fig. 6. It can be observed from Fig. 6 that the increment in D_t for SWS with the increase in C_a by 10° is 46 ms which is comparatively more than the corresponding increment at lower q value and at relatively higher gravity level (0.8 g). For WWS, bubble departure time decreases by 26 ms for increase in C_a by 10°. This elucidates that the increment in heat flux value and reduction in gravity level significantly reduces the D_t for WWS, with the rise in C_a by 10°. It can also be seen from Fig. 6 that the shape of the lower surface of the departed bubble changes from concave shape for surface with C_a of 30° to convex shape for the surface with C_a of 60°.

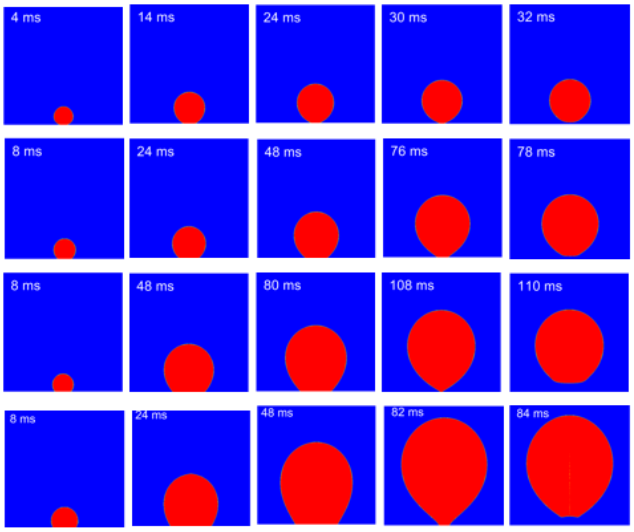

(a) C_a=30°

(b) C_a=40°

(c) C_a=50°

(d) C_a=60°

Fig. 6: Progression of bubble morphology for q of 40 kW/m^2 at gravity level of 0.4 g

3.2 Bubble Equivalent Radius (R_{eq})

Figure 7 presents the growth of the bubble in terms of bubble equivalent radius for surfaces with different wettability at various heat flux values and gravity levels.

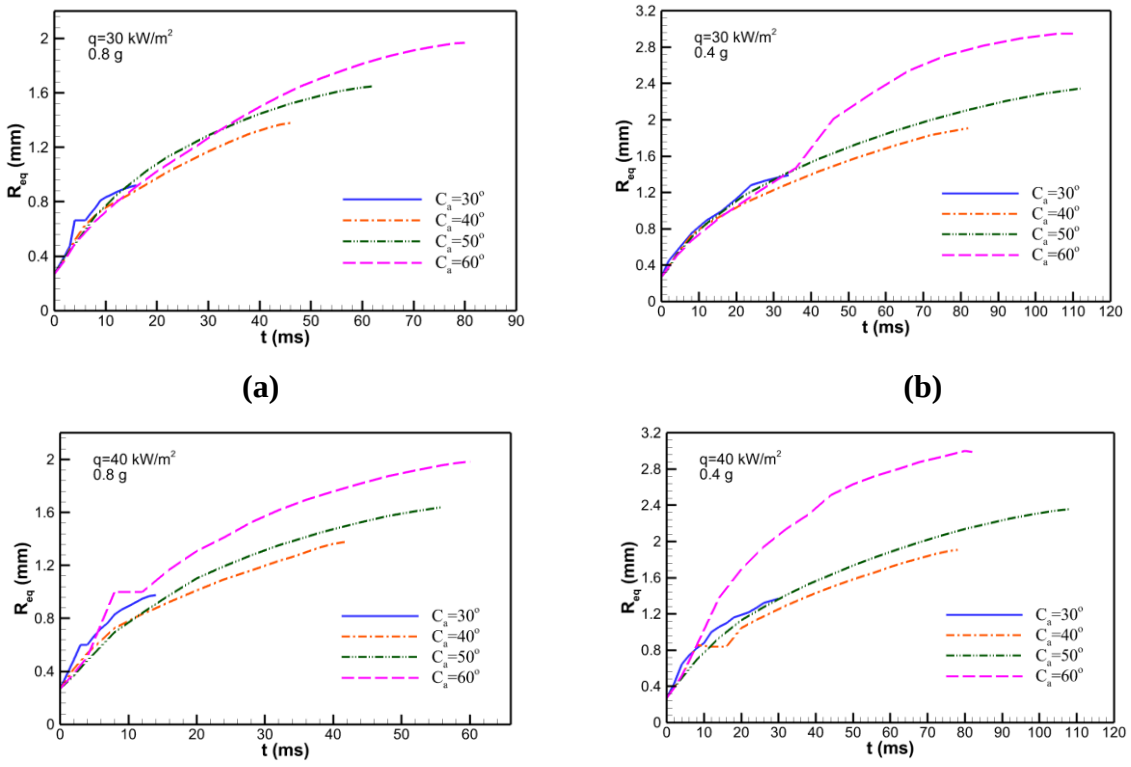

Fig. 7: Variation of bubble equivalent radius (R_{eq}) with time

It can be observed from Fig. 7 (a) that the R_{eq} is more at lower C_a as compared to the higher C_a value during the early stage of the bubble growth. In the late stage before bubble departure, R_{eq} is more for higher C_a. As the gravity level is further reduced for the same q value (Fig. 7 (b)), the effect of variation in C_a in the early stage gets reduced, whereas in the late stage, this effect gets enhanced. From Fig. 7(c), it can be seen that the increment in R_{eq} for surface with lower wettability is comparatively more even in the preliminary period of the growing bubble. This effect gets more magnified as the gravity level is further reduced at higher q value (Fig. 7 (d)). These aspects demonstrate that the effect of increase in heat flux and reduction in gravity level is comparatively more prominent for the surface with lower wettability.

3.3 Bubble Base Radius (B_r)

Modulation of base of the bubble which is in contact with the surface is shown in Fig. 8 for different cases considered in the present study.

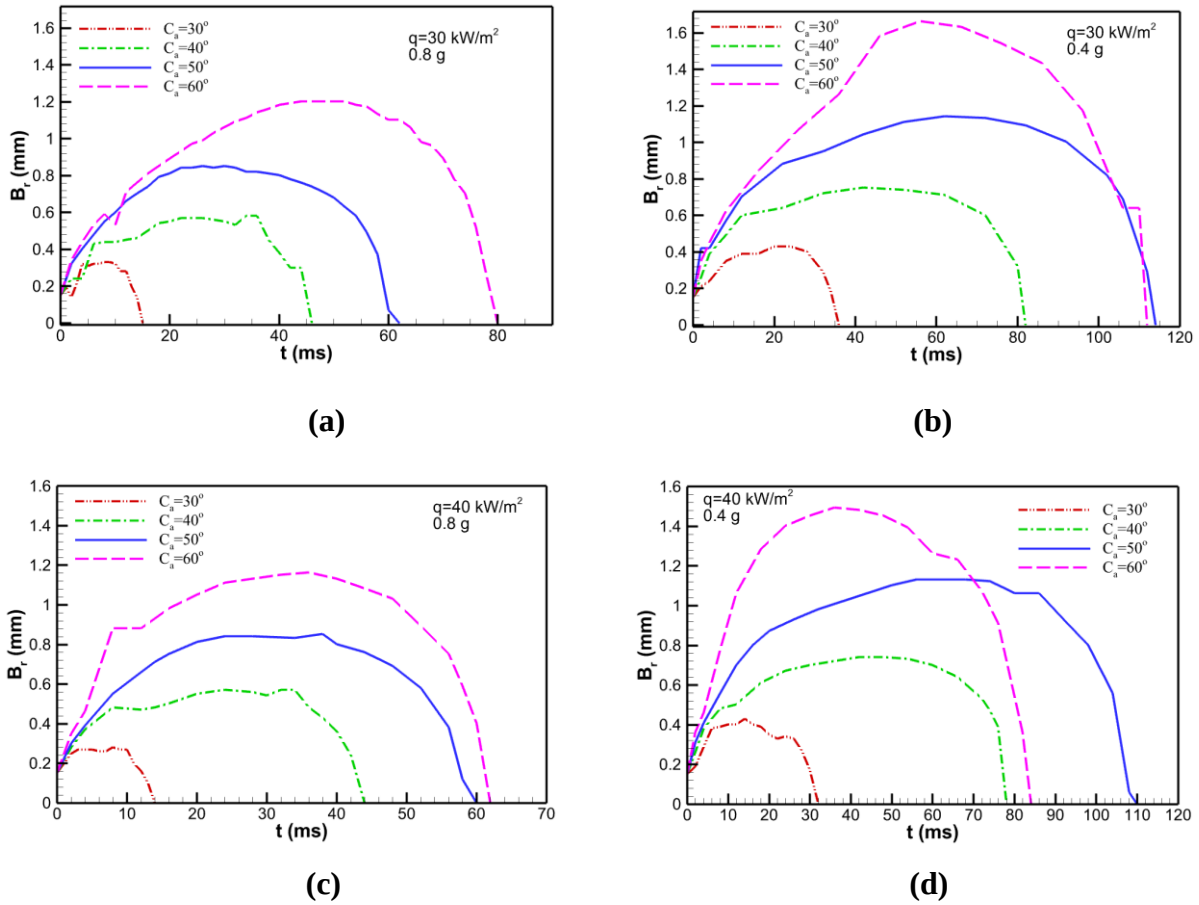

Fig. 8: Variation of bubble base radius (B_r) with time

It can be observed from Fig. 8(a) that the time at which the bubble base radius reaches to its peak value (T_p) are 8 ms, 34 ms, 26 ms and 46 ms for C_a of 30°, 40°,50° and 60°respectively.The increment in peak bubble base radius (B_p) for SWS and WWS is 0.2506 mm and 0.3503 mm with the increase in C_a by 10°. This shows that the rise in T_p is more for SWS whereas the corresponding increment in B_p is more for WWS at lower q (30 kW/m^2)and relatively higher gravity level (0.8 g). From Fig. 8 (b), it is evident that the difference in T_p for SWS and WWS is 22 ms and 6 ms for the change in C_a by 10°. The corresponding increment in B_p is 0.3208 mm and 0.5212 mm, respectively for SWS and WWS. On comparing Figs. 8(a) and 8(b), it can be stated that the effect of reduction in gravity at lower q value is more prominent for WWS. Fig. 8(c) shows that

the increment in B_p is nearly same for both WWS and SWS. The value of T_p increases by 24 ms for SWS, whereas it decreases by 2 ms for WWS with 10° rise in C_a. Figs. 8(a) and 8(c) elucidate that the difference in B_p with surface modulation increases for SWS, but for WWS, it decreases at higher q value under the same gravity levels. It can be seen from Fig. 8 (d) that the increment in B_p is 0.307 mm and 0.361 mm for SWS and WWS, respectively. As far as T_p is concerned, then it is found that the value of T_p decreases by 20 ms for WWS with 10° rise in C_a. On making a comparison between Figs. 8(b) and 8(d), it can be stated that the change in T_p is more at a higher heat flux value, whereas the corresponding change in B_p is more at a lower heat flux for WWS.

4. Conclusion

Numerical computation is performed to investigate the effect of wettability modulation on NPB at various gravity levels and heat flux values. The wettability of the surface is modulated by altering the C_a between the bubble and the surface. It is found that the growth time of the bubble for WWS ($45° < C_a < 90°$) under relatively low gravity conditions (0.4 g) decreases with the deterioration in wettability. This effect gets magnified as the q value is increased. At higher q (40 kW/m^2) under low gravity conditions, the shape of the lower part of the departed bubble changes from concave to convex as the wettability of the surface decreases. With the increase in q value and reduction in gravity level, enhancement in equivalent bubble radius is comparatively more for the surface with lower wettability. Alternation in peak value of bubble base radius with the wettability modulation is comparatively more at lower heat flux (30 kW/m^2) value under relatively lower gravity conditions (0.4 g) for both weakly ($45° < C_a < 90°$) and strongly wetted surfaces ($C_a < 45°$).

References

[1] R. C. Lee, J. E. Nydahl, "Numerical Calculation of Bubble Growth in Nucleate Boiling From Inception Through Departure," *J. Heat Transfer,* vol. 111, no. 2, pp. 474-479, 1989.

[2] Son, Gihun, Vijay K. Dhir, and N. Ramanujapu, "Dynamics and Heat Transfer Associated With a Single Bubble During Nucleate Boiling on a Horizontal Surface," J. Heat Transfer, vol. 121, no. 3, pp. 623-631, 1999.

[3] H. S. &. D. V. K. Abarajith, "A Numerical Study of the Effect of Contact Angle on the Dynamics of a Single Bubble During Pool Boiling," in ASME International Mechanical Engineering Congress & Exposition, New Orleans, Louisiana, 2008.

[4] Wu, J., & Dhir, V. K., "Numerical simulations of the dynamics and heat transfer associated with a single bubble in subcooled pool boiling," Journal of heat transfer, vol. 132, no. 11, p. 111501, 2010.

[5] Wu, Jinfeng, and Vijay K. Dhir, "Numerical Simulation of Dynamics and Heat Transfer Associated With a Single Bubble in Subcooled Boiling and in the Presence of Noncondensables," J. Heat Transfer, vol. 133, no. 4, p. 041502, 2011 .

[6] Gong, S., & Cheng, P., "Lattice Boltzmann simulations for surface wettability effects in saturated pool boiling heat transfer," International Journal of Heat and Mass Transfer, vol. 85, pp. 635-646, 2015.

[7] Pandey, V., Biswas, G., Dalal, A. and Welch, S.W, "Bubble Lifecycle During Heterogeneous Nucleate Boiling," J. Heat Transfer., vol. 140, no. 12, p. 121503 , 2018.

[8] Hirt, C. W., & Nichols, B. D. , "Volume of fluid (VOF) method for the dynamics of free boundaries," Journal of Computational Physics, vol. 39, no. 1, pp. 201-225, 1981.

[9] Brackbill, J. U., Kothe, D. B., & Zemach, C., "A continuum method for modeling surface tension," Journal of Computational Physics, vol. 100, no. 2, pp. 335-354, 1992.

[10] Cooper, M. G., & Lloyd, A. J. P., "The microlayer in nucleate pool boiling," International Journal of Heat and Mass Transfer, vol. 12, no. 8, pp. 895-913, 1969.

[11] Allred, T. P., Weibel, J. A., & Garimella, S. V, "Enabling Highly Effective Boiling from Superhydrophobic Surfaces," *Physical Review Letters,* vol. 120, no. 17, p. 174501, 2018.

[12] Allred, T. P., Weibel, J. A., & Garimella, S. V., "The Role of Dynamic Wetting Behavior during Bubble Growth and Departure from a Solid Surface," *International Journal of Heat and Mass Transfer,* vol. 172, p. 121167, 2021.